

# Effect of Microstructure on the Electrical Properties of Nano-Structured TiN Coatings Deposited by Vacuum Cold Spray

Y.-Y. Wang, Y. Liu, G.-J. Yang, J.-J. Feng, and K. Kusumoto

(Submitted March 9, 2010; in revised form July 8, 2010)

TiN coatings on  $\text{Al}_2\text{O}_3$  substrates were fabricated by vacuum cold spray (VCS) process using ultrafine starting ceramic powders of 20 nm in size at room temperature (RT). Microstructure analysis of the samples was carried out by scanning electron microscopy, transmission electron microscopy, and x-ray diffraction. Sheet resistance of the VCS TiN coatings was measured with a four-point probe. The effects of microstructure on the electrical properties of the coatings were investigated. It was found that the sheet resistance and electrical resistivity of TiN coatings were significantly associating with the spray distance, nozzle traversal speed, and deposition chamber pressure. A minimum sheet resistance of  $127 \Omega$  was achieved. The microstructural changes can be correlated to the electrical resistivity of TiN coatings.

**Keywords** electrical resistivity, microstructure, TiN coating, vacuum cold spray

## 1. Introduction

Vacuum cold spray (VCS) is a novel and promising spray technology developed at the turn of this century. In this process, ultrafine sub-micro-sized ceramic particles are accelerated up to a very high velocity by a carrier gas through a micro-orifice nozzle and subsequently impact and form a coating onto a substrate in a vacuum chamber at room temperature (RT). As the solid ceramic powder is mixed with carrier gas to form an aerosol flow, the technique is also called aerosol deposition (AD) method (Ref 1, 2). Attractive advantages the deposition technology are as follows: (1) during the whole deposition, ceramics in solid state can be deposited onto a ceramic, metallic, or polymer substrate at RT. Consequently, the microstructure of the ceramic powder can be retained without any crystal grain growth or structural changes. This is especially very important for nano-sized or nano-structured ceramic powders. (2) Deposition rate of the VCS process when ceramic powder is used as feedstock

This article is an invited paper selected from presentations at the 4th Asian Thermal Spray Conference (ATSC 2009) and has been expanded from the original presentation. ATSC 2009 was held at Nanyang Hotel, Xi'an Jiaotong University, Xi'an, China, October 22-24, 2009, and was chaired by Chang-Jiu Li.

**Y.-Y. Wang, Y. Liu, G.-J. Yang, and J.-J. Feng**, State Key Laboratory for Mechanical Behavior of Materials, Xi'an Jiaotong University, Shaanxi 710049, China; and **K. Kusumoto**, Department of Mechanical Systems Engineering, Engineering Faculty of Gunma University, Gunma 376-0052, Japan. Contact e-mail: wangyy@mail.xjtu.edu.cn

can reach up to several microns to dozens of microns per minute, which is much faster than other deposition techniques for ceramic films such as sol-gel, sputtering, metal-organic chemical vapor deposition (MO-CVD), and ion-beam deposition. Therefore, VCS technology has many advantages compared with conventional ceramic film and coating deposition methods or thermal spray methods in fabrication of ceramic coatings with thickness ranged from several microns to 100  $\mu\text{m}$ . VCS was used to deposit  $\text{Pb}(\text{Zr},\text{Ti})\text{O}_3$ ,  $\text{Y}_2\text{O}_3$ ,  $\text{YSZ}$ ,  $\text{Al}_2\text{O}_3$ ,  $\text{BaTiO}_3$ ,  $\text{SrTi}_{0.7}\text{Fe}_{0.3}\text{O}_{3-\delta}$ , and other ceramic coatings with nanocrystalline structure, high transparency, high hardness, and high-breakdown voltage at RT (Ref 3-8). In our laboratory, this method was applied to form a nano-sized  $\text{TiO}_2$  coating integrated in a dye-sensitized solar cell system (Ref 9).

TiN is a new multifunctional synthetic cermet material with high strength, high hardness, low friction coefficient, good electrical conductivity, and thermal conductivity. Especially, TiN is a good conductive ceramic with a very low electrical resistivity of  $10^{-7} \Omega \text{ m}$  at RT. It can be used as diffusion barrier layer in microelectronics. TiN films were generally deposited by chemical vapor deposition (CVD) (Ref 10, 11), reactive sputtering (Ref 12, 13), and metal-plasma immersion ion implantation (Me-PIII) (Ref 14). However, one of the shortcomings associating with these processes is the very low deposition rate, apart from the significantly varied ratio of Ti/N depending on deposition conditions. It is difficult to control the chemical compositions and structure of the as-deposited TiN films and subsequently their electrical properties might be deteriorated. Even though Zhang et al. (Ref 10) reported that CVD TiN films on glass substrates achieved a resistance of  $186.7 \Omega$ , it is still likely that the electrical property of the TiN films can be further improved through optimizing film deposition process.

In this study, nano-sized TiN powder was deposited by VCS onto  $\alpha\text{-Al}_2\text{O}_3$  substrates under different spray

conditions. The effects of microstructure on the electrical properties of VCS TiN coatings were investigated.

## 2. Experimental Materials and Procedures

### 2.1 Materials

TiN powder of 20 nm in diameter was used as feedstock. Figure 1 shows the morphology of the powder, which presents a near spherical shape and a relatively narrow granularity distribution about 20-30 nm. The superfine TiN powder shows black.

An  $\alpha$ -Al<sub>2</sub>O<sub>3</sub> plate was used as the substrate. The size is 50 × 20 × 1 mm<sup>3</sup>. Prior to spraying, all Al<sub>2</sub>O<sub>3</sub> plates were ultrasonically cleaned in acetone solution.

### 2.2 VCS TiN Coating Preparation

VCS coating was deposited using VCS-2000 system developed in Xi'an Jiaotong University. A detailed schematic diagram of the spray system was given elsewhere (Ref 9). The system consists of a vacuum deposition chamber, a set of vacuum pumps, an aerosol generation room, an accelerating carrier gas unit, a vibration system to mix the powder with the carrier gas, and a control unit. The deposition chamber contains a micro nozzle, a substrate holder, and a two-dimension worktable. A rotary vane vacuum pump coupled to a mechanical booster is used to pump down the chamber to a pressure of about 100-5000 Pa during spraying. Pure helium gas is used as the powder feeding and accelerating gas. Spray parameters are shown in Table 1. The average powder feed rate is about 0.04 g/min. The deposition efficiency is up to 15-20% according to the spray parameters.

### 2.3 Coating Characterization

Cross-sectional morphologies and fracture behaviors of the TiN coatings were examined by scanning electron microscopy (SEM) (TESCAN-VEGAIIXMU, Czech).

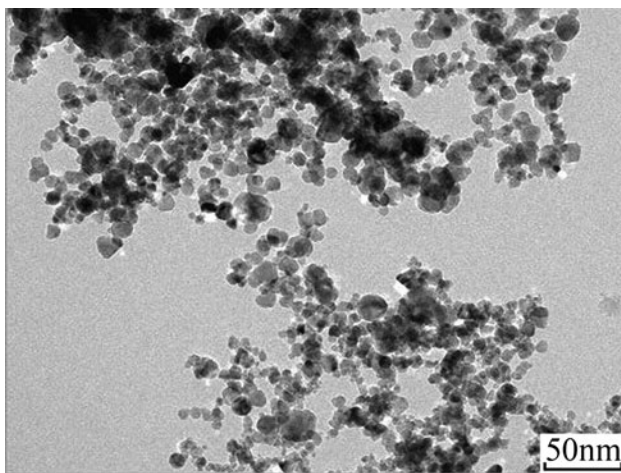


**Fig. 1** Morphology of nano-sized TiN powders

Crystal structure of the coatings and original powders was determined by x-ray diffraction (XRD) (Rigaku-D/max2400, Japan) with a Cu  $K_{\alpha}$  ( $\lambda=1.5405 \text{ \AA}$ ) radiation at 40 kV and 100 mA. A scanning rate of 2°/min was used for diffraction angle 20.

Sheet resistance of the VCS TiN coatings was characterized by four-point probe method (RTS-9, China). The spacing of two adjacent probes is  $1 \pm 0.01 \text{ mm}$ . The probes are made of tungsten carbides with a tiny point of 0.5 mm in diameter.

The electrical resistivity of coatings was obtained according to the relationship between sheet resistance and resistivity of the coatings.

## 3. Results

### 3.1 Crystal Structure of VCS the TiN Coatings

Figure 2 shows the XRD patterns of the original powders and the VCS TiN coatings. It is clear that the two XRD lines are perfectly matched. Peak broadening due to nano-sized crystal grains in the powders does not disappear and no new peak appears. This indicates that the nano-structure of the ceramic powder can be retained in the as-deposited coating without any crystal grain growth or structural changes. This can be attributed to the RT deposition during which the ceramic particles are in solid state.

**Table 1** Spray parameters of VCS process

Deposition chamber pressure, Pa	100, 200, 400, 600, 1000, 5000
Aerosol room pressure, Pa	$2 \times 10^4$
He gas flow, L/min	3
Spray distance, mm	2, 4, 6
Nozzle traversal speed, mm/s	1, 3, 5
Nozzle orifice size, mm	$2.5 \times 0.25$
Deposition temperature	RT

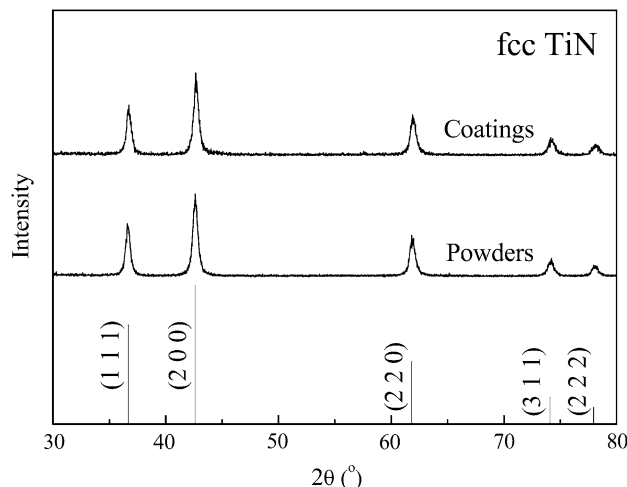


**Fig. 2** XRD patterns of the original powders and VCS TiN coatings

### 3.2 Effect of Spray Passes on the Thickness of the VCS TiN Coatings

When the deposition chamber pressure was kept at 100 Pa, the spray distance was 4 mm, and the traversal speed of nozzle was 5 mm/s, the thickness of the VCS TiN coatings increases linearly with the number of spray passes (Fig. 3). It is indicated that the coating thickness can be regulated through controlling the spray passes. In this study, the TiN coatings of several microns to 200  $\mu\text{m}$  in thickness were successfully fabricated with considerably high deposition rate.

### 3.3 Effect of Spray Distance on the Deposition Rate of the VCS TiN Coatings

The deposition rate of VCS TiN coatings is significantly decreased with the increase in spray distance when the deposition chamber pressure was 100 Pa and the nozzle traversal speed was kept at 5 mm/s (as shown in Fig. 4).

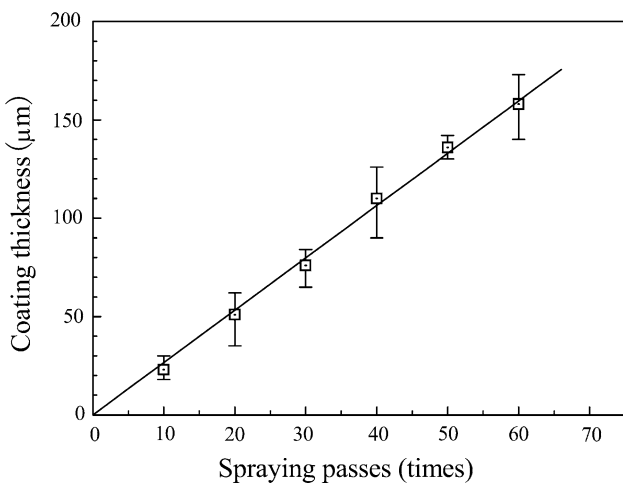


**Fig. 3** Effect of spray passes on the thickness of VCS TiN coatings

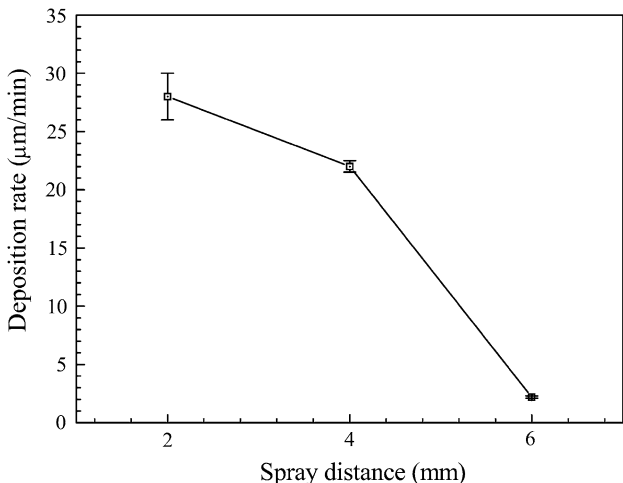


**Fig. 4** Effect of spray distance on the deposition rate of VCS TiN coatings



In this case, the maximum deposition rate at the spray distance of 2 mm reaches 28  $\mu\text{/min}$ , which is near 13 times higher than that at the spray distance of 6 mm. This shows that the deposition efficiency of the coatings is decreased with increasing the spray distance.

### 3.4 Effect of Nozzle Traversal Speed on the Deposition Rate of the VCS TiN Coatings

The deposition rate of the VCS TiN coatings first increases with decreasing the nozzle traversal speed at the spray distance of 6 mm and under the deposition chamber pressure of 100 Pa, and then decreases with further decreasing the nozzle traversal speed (as shown in Fig. 5).

### 3.5 Effect of Deposition Chamber Pressure on the Sheet Resistance of the TiN Coatings

With the increase in the deposition chamber pressure, it was more difficult to deposit a thicker coating under the other spray parameters unchanged. Table 2 shows that the sheet resistance of the coatings with thickness of about 15  $\mu\text{m}$  increases with increasing the chamber pressure. When the chamber pressure is over 600 Pa, the sheet resistance exceeds the maximum range of the four-point-probe apparatus RTS-9.

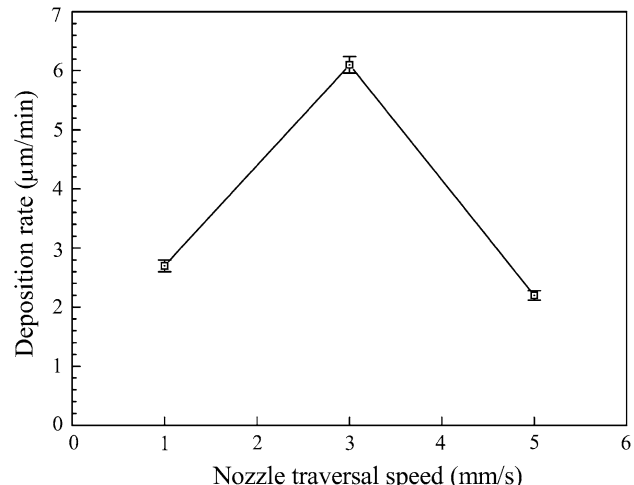


**Fig. 5** Effect of nozzle traversal speed on the deposition rate of VCS TiN coatings

**Table 2** Sheet resistance of TiN coatings vs. deposition chamber pressure

Deposition chamber pressure, Pa	Sheet resistance, $\Omega$
100	5323
200	21,248
400	73,692
600	$>10^6$
1000	$>10^6$
5000	$>10^6$

### 3.6 Effect of Coating Thickness on the Sheet Resistance of the TiN Coatings

The sheet resistance of the VCS TiN coatings remarkably reduces from  $13.6 \text{ k}\Omega$  to  $127 \Omega$  with increasing the coating thickness when the chamber pressure was 100 Pa, the spray distance 6 mm, and the nozzle traversal speed 5 mm/s (as shown in Fig. 6). The minimum sheet resistance of the VCS TiN coating is lower than that of the TiN film deposited by CVD reported by Zhang et al. (Ref 10).

### 3.7 Effect of Spray Distance and Nozzle Traversal Speed on the Electrical Resistivity of the TiN Coatings

The electrical resistivity of the TiN coatings is dramatically decreased from  $0.18$  to  $3 \times 10^{-3} \Omega \text{ m}$  with increasing the spray distance, when the deposition chamber pressure was 100 Pa and the nozzle traversal speed was at 5 mm/s (as shown in Fig. 7).

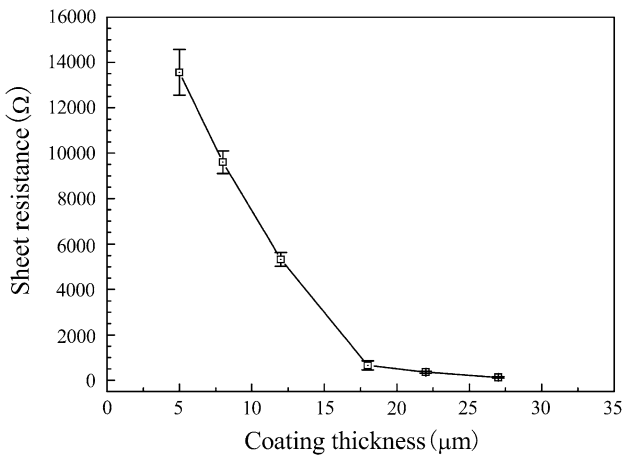


**Fig. 6** Effect of coating thickness on the sheet resistance of VCS TiN coatings

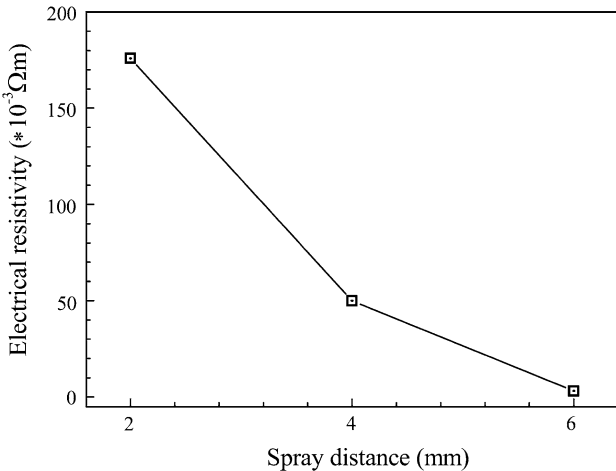


**Fig. 7** Effect of spray distance on the electrical resistivity of VCS TiN coatings

Figure 8 shows that the electrical resistivity of TiN coatings significantly increases up to  $0.46 \Omega \text{ m}$  as the nozzle traverses slower.

## 4. Discussion

### 4.1 Microstructure Features of the VCS TiN Coatings Fabricated with Agglomerated Nano-crystalline Powders and the Deposition Behaviors of Spray Particles

At present, two kinds of starting ceramic powders are usually used to deposit coatings by VCS process. One is compact sintered ceramic powders of submicron, and the other is loose agglomerated ceramic powders of nanocrystalline. When the former is deposited onto a substrate, the fine dense particles of high velocity collide with the substrate and fracture due to the brittle feature of the ceramic material. Therefore, the high kinetic energy owing to the high velocity promotes the bonding between the particles and the substrate, and between the particles. This is so-called RT impact consolidation (RTIC) (Ref 4).

When ceramic powders of dozens of nanometers in diameter are used as feedstock in VCS process, these ultrafine grains tend to agglomerate and form relatively large and porous submicron granules both in the aerosol room and in-flight due to the high specific surface energy of nano-sized grains. The loose agglomerated particles successively impact on the substrate and subsequently severely deform due to their porous structure to form the first layer. Then the following particles of high velocity collide with the pre-deposited coatings, which further make the former layer considerably denser due to “tamping effect” (Ref 15).

However, the detailed bonding mechanisms of VCS coating has not been fully illuminated yet.

Figure 9 shows a typical cross-sectional microstructure of VCS TiN coatings with a magnification of 50k. It is

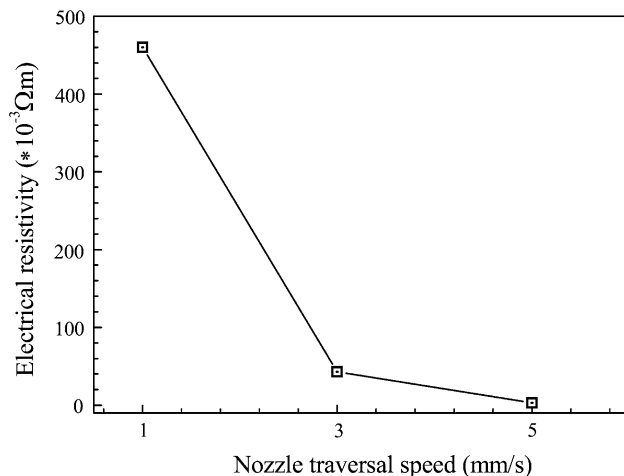


**Fig. 8** Effect of nozzle traversal speed on the electrical resistivity of VCS TiN coatings

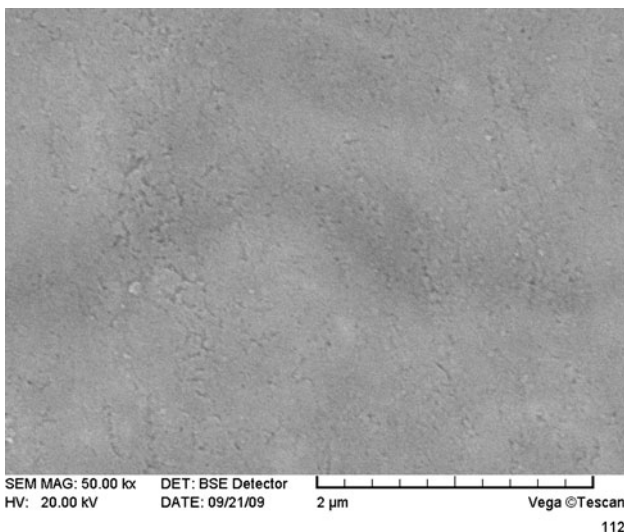


**Fig. 9** Typical cross-sectional microstructure of VCS TiN coatings

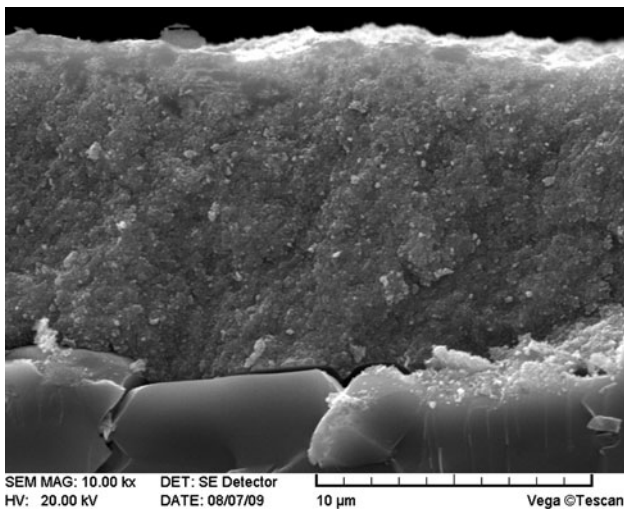


**Fig. 10** Typical fractograph of VCS TiN coatings

found that the coating has a considerably dense structure and pores or gaps of size more than 100 nm between particles in the coating can hardly be observed. However, pores or gaps of dozens of nanometers in size between particles still exist. It is indicated that there exist bonding forces to some extent between the nano-crystalline grains and agglomerated particles.

Figure 10 shows a typical fractograph of the VCS TiN coatings. The coatings were deposited on the  $\alpha$ -Al<sub>2</sub>O<sub>3</sub> substrate and then were fractured by external force for characterization. It is found that the coatings present good adhesion to the substrate.

As the ultrafine ceramic particles are accelerated and then impact onto the substrate to form the coating at RT, not all of the particles will be deposited onto the



substrate to form coatings. It strongly depends on the critical velocity of the particles before impacting on the substrate or the pre-coating. Only the particles with a velocity higher than the critical value will be deposited. Otherwise, they cannot form coatings. Moreover, the deposited coating presents denser structure with increasing the velocity of the spray particles due to their higher kinetic energy. However, when the velocity of the particles exceeds a certain value, erosion of these particles to the substrate surface and the deposited coating occurs.

Although the effects of spray distance on the velocity of particles are not directly illuminated by experiment, it may be deduced that the particle velocity will increase with increasing the spray distance ranged from 2 to 6 mm according to the coating thickness data (Fig. 4) combined with the experimental results concerning the electrical properties of the VCS TiN coatings (shown in Fig. 7). The reason of the decreased deposition rate with the increased spray distance (as shown in Fig. 4) is that the spray erosion becomes more serious with the increase of particle velocity as mentioned above. On the other hand, the tamping effect is enhanced due to the high velocity. Therefore, the cohesion between the ultrafine particles in the coating is enhanced and consequently the coating becomes denser with the increase in the spray distance.

The lower nozzle traversal speed implies more particles impacting a certain point on the substrate simultaneously. Therefore, the deposition rate increases when the nozzle traverses slightly slower. With the nozzle traversal speed further reducing, the deposition rate decreases instead (as shown in Fig. 5). This is because a thicker layer deposited after one spray pass leads to the tamping effect of the subsequent particles significantly impaired. In consequence, the cohesion between the thicker layers and particles in the layers is seriously weakened. Figure 11 shows the cross-sectional structure of the TiN coatings deposited at the nozzle traversal speed of 5 and 1 mm/s, respectively. It is clear that obvious lamella structure (dark line in Fig. 11b) can be found.

#### 4.2 Effects of Microstructure on the Electrical Properties of VCS TiN Coatings

TiN crystals belong to a face-centered cubic lattice (as shown in Fig. 2) and are put together by covalent bond and metallic bond. The electrical conductivity of bulk TiN primarily depends on the free electron in the sub-outer orbit 3d of Ti atom. Due to a large number of free electrons existing in bulk TiN, TiN has a very low resistivity about  $10^{-7} \Omega \text{ m}$  order of magnitude (Ref 16). However, there are plenty of defects such as porosities and non-bonding gaps in the VCS coatings. Accordingly, the resistance of the free electron migration in the coatings remarkably rises. Therefore, the coating resistivity significantly increases. As the mean free path of He gas molecules becomes shorter with increasing the deposition chamber pressure, the ultrafine particles run into more gas drag. Accordingly, the velocity of the spray particles dramatically decreases. As a result, the deposited TiN

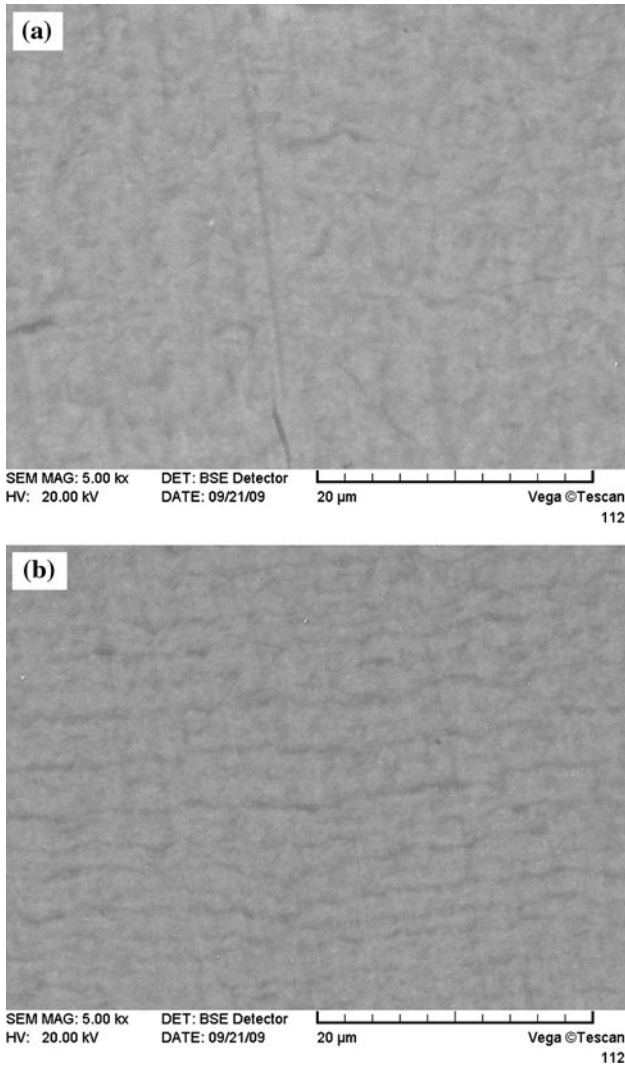


**Fig. 11** Cross-sectional microstructure of VCS TiN coatings (nozzle traversal speed: (a) 5 mm/s and (b) 1 m/s)

coatings present higher porosity and more gaps (Ref 17). The electrons transfer in the coatings with a large number of defects will encounter great resistance. Therefore, the sheet resistance of the coatings increases with increasing the chamber pressure.

According to Fig. 3, the increase in coating thickness means more spray passes. It is implied that the tamping effect is enhanced with increasing coating thickness. Consequently, the coatings become denser and porosities and gaps in the coatings significantly turn to be lower. As a result, the sheet resistance of VCS TiN coatings remarkably reduces with the increase in the coating thickness (as shown in Fig. 6). Due to the same reasons mentioned above, the electrical resistivity of the TiN coatings is dramatically decreased with the increase in the spray distance and significantly increases with the decrease in the nozzle traversal speed.

## 5. Conclusions

TiN coatings with thickness of several microns to 200  $\mu\text{m}$  were successfully fabricated by VCS process using ultrafine ceramic powders of 20 nm in size at RT. The deposition rate varied with the spray distance, nozzle traversal speed, and deposition chamber pressure and reached up to 28  $\mu\text{m}/\text{min}$ . The sheet resistance of the VCS TiN coatings was significantly reduced with decreasing the deposition chamber pressure and increasing the spray passes or the coating thickness. The minimum sheet resistance of 127  $\Omega$  was obtained under the present spray conditions. The electrical resistivity of the VCS TiN coatings remarkably decreased with the increase in the spray distance and the increase in the nozzle traversal speed. A minimum electrical resistivity of  $3 \times 10^{-3} \Omega \text{ m}$  was achieved.

## Acknowledgment

The project was supported by National Natural Science Foundation of China (Contract No.: 50705075).

## References

1. M. Levedev, J. Akedo, K. Mori, and T. Eiju, Simple Self-Selective Method of Velocity Measurement for Particles in Impact-Based Deposition, *J. Vac. Sci. Technol. A*, 2000, **18**(2), p 563-566
2. J. Akedo and M. Lebedev, Microstructure and Electrical Properties of Lead Zirconate Titanate (Pb(Zr52/Ti48)03) Thick Film Deposited with Aerosol Deposition Method, *Jpn. J. Appl. Phys.*, 1999, **38**(9B), p 5397-5401
3. J. Akedo, Aerosol Deposition Method for Fabrication of Nano Crystal Ceramic Layer—Novel Ceramics Coating with Collision of Fine Powder at Room Temperature, *Mater. Sci. Form.*, 2004, **449-452**, p 43-48
4. J. Akedo, Room Temperature Impact Consolidation (RTIC) of Fine Ceramic Powder by Aerosol Deposition Method and Applications to Microdevices, *J. Therm. Spray Technol.*, 2008, **17**(2), p 181-198
5. H.J. Kim, Y.J. Yoon, J.H. Kim, and S.M. Nam, Application of Al<sub>2</sub>O<sub>3</sub>-Based Polyimide Composite Thick Films to Integrated Substrates Using Aerosol Deposition Method, *Mater. Sci. Eng. B*, 2009, **161**, p 104-108
6. J.M. Oh, N.H. Kim, S.C. Choi, and S.M. Nam, Thickness Dependence of Dielectric Properties in BaTiO<sub>3</sub> Films Fabricated by Aerosol Deposition Method, *Mater. Sci. Eng. B*, 2009, **161**, p 80-84
7. K. Sahner, M. Kaspar, and R. Moos, Assessment of the Novel Aerosol Deposition Method for Room Temperature Preparation of Metal Oxide Gas Sensor Films, *Sens. Actuators B*, 2009, **139**, p 394-399
8. J.-J. Choi, B.-D. Hahn, J. Ryu, W.-H. Yoon, B.-K. Lee, and D.-S. Park, Preparation and Characterization of Piezoelectric Ceramic-Polymer Composite Thick Films by Aerosol Deposition for Sensor Application, *Sens. Actuators A*, 2009, **153**, p 89-95
9. S.-Q. Fan, G.-J. Yang, G.-J. Liu, C.-X. Li, C.-j. Li, and L.-Z. Zhang, Characterization of Microstructure of TiO<sub>2</sub> Coating Deposited by Vacuum Cold Spraying, *J. Therm. Spray Technol.*, 2006, **15**(4), p 513-517
10. T. Zhang, G. Zhao, and G. Han, Growth and Properties of TiN Films on Glass by Atmospheric Pressure Chemical Vapor Deposition, *J. Vac. Sci. Technol.*, 2005, **25**(4), p 309-311



11. L. Yi, W.j. Zhang, and J. Wu, Study of Metal Organic Chemical Vapor Deposition Tin Thin Films in Real Structures, *Thin Solid Films*, 2006, **515**, p 2803-2806
12. M. Popovic, M. Stojanovic, D. Perusko et al., Ion Beam Modification of Structural and Electrical Properties of Tin Thin Films, *Nucl. Instrum. Methods B*, 2008, **266**, p 2507-2510
13. M. Nose, T. Nagae, M. Yokota, S. Saji, M. Zhou, and M. Nakada, Electrical and Colorimetric Properties of Tin Thin Films Prepared by DC Reactive Sputtering in a Facing Targets Sputtering (FTS) System, *Surf. Coat. Technol.*, 1999, **116-119**, p 296-301
14. P. Huber, D. Manova, S. Mandl, and B. Rauschenbach, Optical Characterization of Tin Produced by Metal-Plasma Immersion Ion Implantation, *Surf. Coat. Technol.*, 2001, **142-144**, p 418-423
15. P.-H. Gao, Y.-G. Li, C.-J. Li, G.-J. Yang, and C.-X. Li, Influence of Powder Porous Structure on the Deposition Behavior of Cold-Sprayed WC-12Co Coatings, *J. Therm. Spray Technol.*, 2008, **17**(5-6), p 742-749
16. Y. Ren-hong and J. Ming-xue, Properties and Applications of TiN and Techniques of Powder Preparation, *Refractories*, 2005, **36**(5), p 386-389 (in Chinese)
17. L. Kai-Xing, "Influence of Powder Structure and Accelerating Gas Flow on Electron Transport Property of Nanostructured TiO<sub>2</sub> Films Deposited by Vacuum Cold Spray", Master Thesis, Xi'an Jiaotong University, May 2010, p 28-31